# Functional Characterization of the Native NH 2 -Terminal Transactivation Domain of the Human Androgen Receptor: Binding Kinetics for Interactions with TFIIF and SRC-1a †

**2 AUTHORS**, INCLUDING:

Iain J Mcewan
University of Aberdeen
**89** PUBLICATIONS **2,469** CITATIONS

# Functional Characterization of the Native NH$_2$-Terminal Transactivation Domain of the Human Androgen Receptor: Binding Kinetics for Interactions with TFIIF and SRC-1a[†]

Derek N. Lavery[‡] and Iain J. McEwan*

*School of Medical Sciences, Institute of Medical Sciences, University of Aberdeen, Foresterhill, Aberdeen AB25 2ZD, United Kingdom*

ABSTRACT: The androgen receptor (AR) is a ligand-activated transcription factor that mediates the actions of the steroid hormones testosterone and dihydrotestosterone at the level of gene transcription. The main transactivation function is modular in structure, maps to the N-terminal domain (NTD), and is termed AF1. This region of the AR is structurally flexible and functions in multiple protein–protein interactions with coregulatory proteins and components of the general transcription machinery. Using surface plasmon resonance, the binding kinetics for the interaction of AR-AF1 with the large subunit of the general transcription factor TFIIF, termed RAP74, and the coactivator SRC-1a were measured. AR-AF1 interacts with both the NTD and CTD of RAP74 and the CTD of SRC-1a. The dissociation constants ($K_d$) for the binding of polypeptides derived from RAP74 are in the submicromolar range, while a peptide from SRC-1a bound with a $K_d$ of 14 $\mu$M. Significantly, the individual NTD and CTD of RAP74 interacted with AR-AF1 with distinct binding kinetics, with the NTD exhibiting slower on and off rates. TFIIF is involved in transcription initiation and elongation, and the CTD of RAP74 binds to the RNA polymerase II enzyme, the general transcription factor TFIIB, and a CTD phosphatase, FCP1. We have mutated hydrophobic residues in the RAP74-CTD structure to disrupt secondary structure elements and show that binding of AR-AF1 depends upon helix 3 in the winged-helix domain of the RAP74-CTD polypeptide. Altogether, a model is suggested for AR-AF1-dependent transactivation of receptor−target genes.

The androgen receptor (AR)[1] is a member of the steroid hormone receptor (SHR) subfamily of nuclear receptors, which also includes the estrogen, progesterone, mineralocorticoid, and glucocorticoid receptors. This family of receptors has a modular and well-defined domain organization, with the central and C-terminal domains involved in DNA recognition and ligand binding, respectively. The functions of these domains are well-characterized, and structures for the isolated domains have been determined by X-ray crystallography and/or NMR spectroscopy for nearly all SHRs. The N-terminal domain (NTD), in contrast, appears disordered and structurally flexible and contains residues important for mediating protein–protein interactions necessary for transcription regulation, termed activation function 1 (AF1) (for a review, see ref *1*). In the case of the AR, the main determinants for receptor-dependent gene activation map to the NTD (*2–4*).

The AF1 domain can act as a ligand-independent transactivation domain, when fused directly to a DNA-binding domain (see refs *3*, *5*, and *6*). AR-NTD/AF1 is responsible for interactions with a host of proteins important for transcription regulation (reviewed in ref *1*). Coactivators such as CBP/p300 (*7–9*), SRC/p160 (*10–13*), and components of the general transcription machinery, such as TFIIF (*5, 13*) and TFIIH (*14*), are known to interact with this domain. Also, the binding sites of multiple corepressors have been mapped to the SHR NTD, including NCoR and SMRT (*15*) and a potential AR-selective repressor Hey1 (*16*). We have previously reported the interaction of AR-AF1 with the large subunit of TFIIF, termed RAP74 (*5*), and mapped the receptor binding sites to the NTD and CTD of RAP74 (*13*).

TFIIF is a heterotetramer of two different subunits, RAP30 and RAP74, and is important for transcriptional initiation and elongation (*17–19*). Structural information is available for the NTDs of RAP30 and RAP74, which reveals a unique triple-$\beta$-barrel dimerization surface (*20*). The CTD of RAP74 forms a winged-helix structure and is important for binding to other components of the general transcription machinery (*21–23*).

* To whom correspondence should be addressed: School of Medical Sciences, Institute of Medical Sciences, University of Aberdeen, Foresterhill, Aberdeen AB25 2ZD, Scotland, United Kingdom. Telephone: +44(0)1224-555807. Fax: +44(0)1224-555844. E-mail: iain.mcewan@abdn.ac.uk.

[‡] Present address: Androgen Signalling Laboratory, Department of Oncology, Imperial College London, London, U.K.

[1] Abbreviations: AF-1, activation function 1; AR, androgen receptor; ARE, androgen response element; CBP, CREB binding protein; CTD, C-terminal domain; ER$\alpha$, estrogen receptor $\alpha$; FCP1, RNA polymerase II carboxy-terminal domain phosphatase; GR, glucocorticoid receptor; GST, glutathione *S*-transferase; MID, middle domain; NTD, N-terminal domain; PIC, preinitiation complex; PSA, prostate-specific antigen; RAP30/74, RNA polymerase II-associated protein 30/74; SHR, steroid hormone receptor; SRC, steroid receptor coactivator; TBP, TATA-binding protein.

Given the importance of the AF1 domain for AR action, it is vital to understand the nature of protein–protein interactions that mediate receptor-dependent transactivation and the structural properties of this region. In this study, we have used surface plasmon resonance to investigate the binding kinetics of AR-AF1 with polypeptides derived from the large subunit of TFIIF, RAP74, and a peptide derived from the coactivator protein SRC-1a. We have used structural analysis and site-directed mutagenesis to study the AF1 binding site in the C-terminal domain of RAP74. We describe binding affinities in the submicromolar range for RAP74 polypeptides and highlight the importance of helix 3 in the RAP74-CTD polypeptide for AF1 binding. Together, these finds suggest a mechanism of action for the AR-AF1–TFIIF interaction.

## EXPERIMENTAL PROCEDURES

*Plasmid Construction and Site-Directed Mutagenesis.* The plasmids containing the AF1 domain (amino acids 142–485) of the human AR tagged with histidine or GST and RAP74 (full-length and isolated domains) have been described previously (*24*). The plasmids encoding both full-length (amino acids 1–517) and C-terminal (amino acids 363–517) RAP74 were a kind gift from Z. F. Burton (University of Michigan, Ann Arbor, MI) (*25*) and were used as the parental templates in all mutagenesis reactions. Primers were designed to target hydrophobic residues in helices H1–H3 of the RAP74-CTD polypeptide, via substitution of these with proline residues, and thereby disrupt secondary structure as assessed by prediction algorithms. The mutagenesis primers used were as follows (base pairs mutated are indicated in bold and artificially engineered restriction sites underlined): mH1 (V459P/L463P), forward primer 5′-GGATGCC**C**CGCGC-CGCTACC**C**GACT**C**GGAAGCC-3′ (*Hin*fI site underlined); mH2/2.5 (L474P), forward primer 5′-GGACCTGC**C**CG-AAAAAGTTCCAGACCAAGAAGACAGGC**C**TGAGC-3′, (*Stu*I site underlined); and mH3 (V490P/L493P/L497P), forward primer 5′-GCGAGCAGACA**C**CGAACGT**G**CCG-GCCCAGATCCCCAAGC-3′ (*Nae*I site underlined). The PCR-based mutagenesis reactions were conducted using the Quickchange mutagenesis protocol (Stratagene). To accurately select colonies positive for mutations, a combined PCR and restriction digest approach was employed. First, aliquots of "crude" plasmid preparations were used as template DNA in a PCR (Promega, outlined below). Using T7 sequence-specific primers, only the RAP74 cDNA insert was amplified: T7 forward primer 5′-GTTTCCCTCCTA-GAAA-3′ and T7 reverse primer 5′-CTAGTTATTGCT-CAGC-3′. Samples of the PCR products were digested with mutation-specific restriction enzymes, and fragments were analyzed by 1% agarose electrophoresis. Finally, plasmid DNA for the individual mutations was sequenced to confirm the presence of desired mutations: it was observed that all helical mutants contained a silent mutation (TCT to TCC) at serine 514.

*Bioinformatic Analysis.* Secondary structure predictions for wild-type RAP74 and its mutants were performed on the full-length domains and subdomains of RAP74 using the Network Protein Sequence Analysis (consensus secondary structure prediction) algorithm provided by the Pole Bioinformatique Lyonnais (http://npsa-pbil.ibcp.fr) (*26*).

*Protein Expression and Purification.* Histidine-tagged AR-AF1 (amino acids 142–485), full-length RAP74 (amino acids 1–517), the MID (amino acids 258–356), and the CTD (amino acids 363–517) were expressed in *Escherichia coli* strain BLR(DE3) or BL21(pLysS) for 1.5–2 h by induction with 1 mM isopropyl β-D-thiogalactoside at 37 °C in LB or 2×TY medium. Bacterial cells were pelleted by centrifugation, resuspended in buffer A [20 mM Tris-HCl (pH 7.9), 50 mM NaCl, 1 mM EDTA, 1 mM phenylmethanesulfonyl fluoride, and 1 mM dithiothreitol], and stored at −80 °C. Cell lysis was achieved by freezing and thawing and addition of lysozyme (0.5 mg/mL) at 4 °C. Proteins were purified from the soluble fraction by Ni$^{2+}$-agarose affinity chromatography (Qiagen). The RAP74-NTD polypeptide (amino acids 1–136) is insoluble under these conditions and was purified from inclusion bodies by denaturation with 8 M urea and subsequent Ni$^{2+}$-agarose affinity chromatography (Qiagen). AR-AF1 was dialyzed extensively against 25 mM HEPES (pH 7.9), 100 mM sodium acetate, 5% glycerol, and 1 mM dithiothreitol at 4 °C. RAP74 polypeptides (excluding the RAP74-NTD polypeptide) were dialyzed against 25 mM HEPES (pH 7.9), 250 mM sodium acetate, 5% glycerol, and 1 mM dithiothreitol at 4 °C. The RAP74-NTD polypeptide was dialyzed against the buffer described above but in a stepwise fashion, reducing the concentration of urea in molar amounts at hourly stages. Proteins were assessed for purity by SDS–PAGE and scanning of the stained gels using Image J (NIH). Protein concentrations were estimated using known BSA concentrations using Bradford reagent (Bio-Rad). Aliquots of protein were snap-frozen in liquid N$_2$ and stored at −80 °C until they were used.

*Partial Proteolysis.* To examine the tertiary structure of mutant forms of RAP74 and the RAP74-CTD polypeptide, recombinant proteins were challenged with proteolytic enzymes; 100 μmol of recombinant protein was diluted in proteolysis buffer [25 mM HEPES (pH 7.9), 0.2 mM EDTA, 5 mM MgCl$_2$, 20 mM CaCl$_2$, 60 mM KCl, and 10% glycerol] to give a reaction volume of 10 μL and challenged with 100 ng of endo-Glu C protease or 2 ng of trypsin over a series of time points (see the legend of Figure 4) at room temperature or 30 °C. Reactions were stopped by addition of 2× SDS sample buffer, and samples were heated at 75 °C for 5 min. Samples were resolved by SDS–PAGE on a 12.5 or 15% gel and fragments generated analyzed by silver staining.

*Surface Plasmon Resonance.* Real-time measurements of protein–protein interactions were studied using a Biacore 2000 instrument. AR-AF1 was diluted in sodium acetate buffer (pH 4) to a concentration of 10 μg/mL and immobilized on the CM5 sensor chip surface using the amine coupling kit (Biacore) at a flow rate of 10 μL/min. This procedure resulted in the immobilization of ∼500 relative units (RU) of AR-AF1 to the sensor chip surface. For kinetic studies, small amounts of immobilized protein are preferred as this minimizes the effect of mass transport. To generate binding curves, multiple concentrations of analyte protein were passed over immobilized AR-AF1 at a flow rate of 20 μL/min. The total contact time (or association phase) was ∼160 s, and the dissociation phase was ∼180 s in length. Protein–protein interactions were corrected for the influence of nonspecific interactions by subtracting interactions of analyte proteins with a blank flow cell. Kinetic parameters

of protein–protein interactions were determined using Biaevaluation 3.0 (Biacore) fitted to a 1:1 Langmuir binding model.

*Protein–Protein Binding Studies.* Protein–protein interactions were analyzed on a Scintistrip microtiter 96-well plate (PerkinElmer Life Sciences) utilizing both purified recombinant and in vitro transcribed/translated $^{35}$S-labeled proteins as described previously (*5*). Briefly, control (BSA) or purified AR-AF1 was diluted in chilled (4 °C) binding buffer [20 mM HEPES (pH 7.9), 100 mM KCl, 10% glycerol, 5 mM MgCl$_2$, 0.2 mM EDTA, 5 mM $\beta$-mercaptoethanol, and 0.2 mM PMSF], added to the microtiter plate in triplicate to a final concentration of 200 nM/well, and left to adsorb for 2–3 days at 4 °C. The wells were there incubated with 200 $\mu$L of 5 mg/mL BSA to block nonspecific sites prior to incubation with radiolabeled wild-type or mutant RAP74-CTD polypeptides for 1.5 h at room temperature with gentle shaking. Radiolabeled proteins were synthesized using a rabbit reticulocyte system (Promega) following the manufacturer's instructions. Nonspecific and nonbound radiolabeled proteins were removed with four washes of binding buffer with the addition of 1 mg/mL BSA and specific interactions analyzed by scintillation counting in a Microß counter (PerkinElmer Life Sciences). Interactions between radiolabeled and adsorbed proteins were calculated and normalized against nonspecific binding to control proteins (BSA). Furthermore, wells were stripped with 20 $\mu$L of 1× SDS sample buffer [50 mM Tris-HCl (pH 6.8), 2% SDS, 0.1% bromophenol blue, 10% glycerol, and 10 mM DTT] per well by incubation for 1 h at room temperature. Triplicate samples were pooled, resolved by SDS−PAGE, and analyzed by autoradiography.

## RESULTS

*Binding Kinetics of AR-AF1−Target Protein Interactions.* The binding of AR-AF1 to TFIIF has been shown to be important for receptor-dependent transcription initiation in vitro (*6*) and the binding sites mapped to the NTD and CTD of the large subunit of TFIIF, termed RAP74 (*13*). AR-NTD/AF1 has also been shown to interact with the CTD of the coactivator protein SRC-1a (*11, 13, 27*). However, steady-state binding assays provide limited information regarding the likely importance of specific interactions. To characterize these selected interactions in more detail, we have used surface plasmon resonance to determine the binding kinetics and relative affinities. Panels A and B of Figure 1 show schematic representations of the domain organization of the human AR and RAP74 proteins and recombinant polypeptides used in the biochemical studies below. Proteins were purified from soluble bacterial extracts after overexpression. Figure 1C shows recombinant AR-AF1 and subdomains of RAP74 after Ni affinity chromatography: full-length AR-AF1, RAP74, and RAP74-CTD and -NTD polypeptides were judged to be between 75 and >95% pure, with the exception of the RAP74-MID polypeptide, which was 50% pure. Purified AR-AF1 polypeptide was immobilized on a sensor chip using amine coupling chemistry and titrated with different concentrations of TFIIF polypeptides, RAP74, RAP74-NTD, RAP74-CTD, or a peptide derived from SRC-1a (Q rich box B; see ref *28*). In preliminary studies, the binding of the RAP74-NTD and -CTD polypeptides, but not
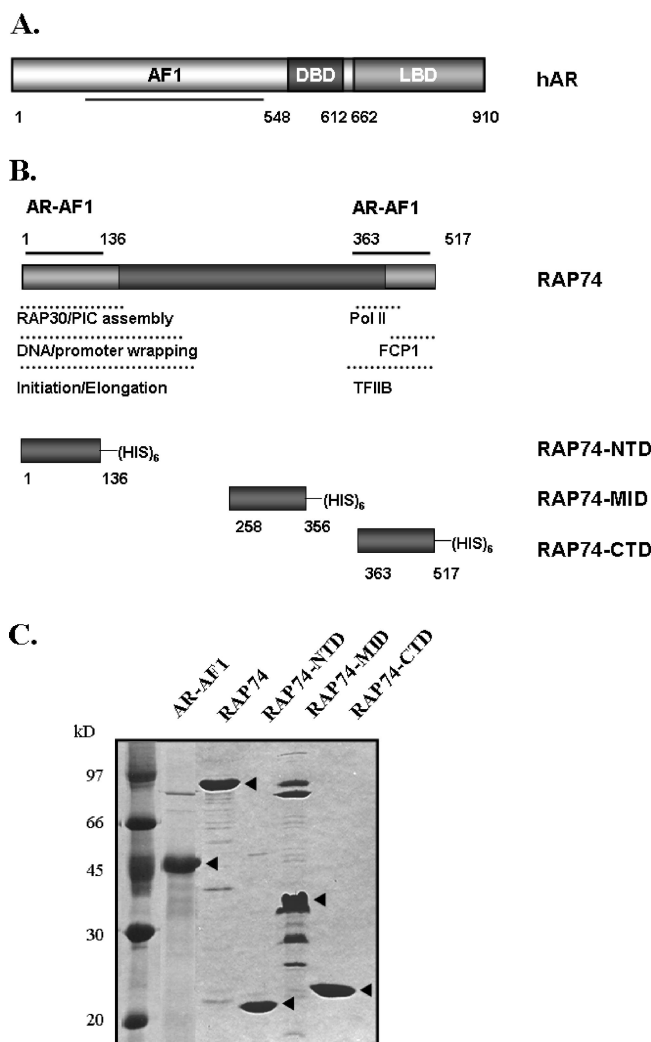


FIGURE 1: Purification of recombinant AR-AF1 and RAP74 polypeptides. (A) Schematic representation of the domain organization of the AR, showing the ligand (LBD) and DNA (DBD) binding domains and the AF1 transactivation domain (amino acids 142−485). (B) Schematic representation of the large subunit of TFIIF, RAP74. The globular N- and C-terminal domains are indicated together with a summary of RAP74 function and protein–protein interactions (see the text for details). The His-tagged recombinant proteins used in binding studies are indicated. (C) Coomassie-stained gel of partially purified recombinant proteins; 2 $\mu$g of AR-AF1, full-length RAP74, and RAP74-NTD, -MID, and -CTD polypeptides were resolved on a 12.5% polyacrylamide gel and stained with Coomassie Blue. Note that the RAP74-MID polypeptide exhibits abnormal mobility as reported previously (*13, 25*).

the middle domain of RAP74, were confirmed at a single analyte concentration (data not shown). Figure 2 shows the sensorgrams generated with the different polypeptides, and from these data, the on rate and off rate for the different interactions were measured. Full-length RAP74 interacted with a slow on and relatively fast off rate and with a relative binding affinity ($K_d$) of 170 nM (Figure 2A and Table 1). The RAP74-NTD and -CTD binding sites showed contrasting binding kinetics. The RAP74-NTD polypeptide bound with slow on and off rates, resulting in a $K_d$ of 290 nM (Figure 2B and Table 1), while the RAP74-CTD polypeptide exhibited relatively fast on and off rates and a $K_d$ of 630 nM (Figure 2C and Table 1). A 40-amino acid peptide from the coactivator SRC-1a exhibited a slow on rate and a fast
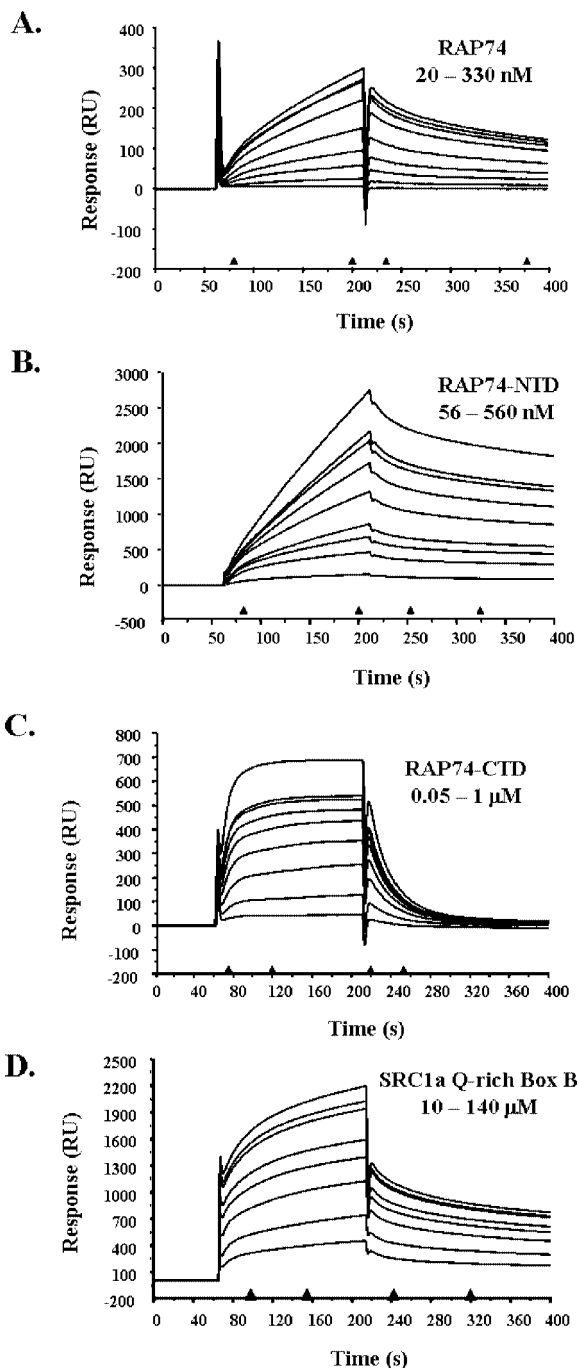
**A.**



**B.**



**C.**



**D.**



FIGURE 2: Binding kinetics of AR-AF1 with partner proteins. (A) Overlaid sensorgrams generated by passing increasing concentrations of RAP74 over immobilized AR-AF1. Concentrations of RAP74 were passed over the sensor chip surface at a flow rate of 20 $\mu$L/min for a total contact time of 150 s. RAP74 concentrations were 20, 40, 80, 120, 170, 210, 250, 290, and 330 nM. (B) Overlaid sensorgrams generated by passing increasing concentrations of the RAP74-NTD polypeptide (56, 140, 210, 280, 350, 420, 460, 520, and 560 nM) over immobilized AR-AF1 at a flow rate of 20 $\mu$L/min for a total contact time of 150 s. (C) Overlaid sensorgrams generated by passing increasing concentrations of the RAP74-CTD polypeptide (50, 130, 250, 380, 500, 630, 750, 880, and 1000 nM) over immobilized AR-AF1 at a flow rate of 20 $\mu$L/min for a total contact time of 150 s. (D) Overlaid sensorgrams generated by passing increasing concentrations of a peptide from SRC-1a (10, 20, 40, 60, 80, 100, 120, and 140 $\mu$M) over immobilized AR-AF1 at a flow rate of 20 $\mu$L/min for a total contact time of 150 s. Linear regions selected for kinetic analysis using BIA evaluation are denoted with filled triangles. All binding curves were repeated and similar results obtained.

Table 1: Binding Kinetics for AR-AF1-Coregulator Interactions

| binding partner | $k_a$, on rate (M$^{-1}$ s$^{-1}$) | $k_d$, off rate (s$^{-1}$) | $K_d$ (M) |
|---|---|---|---|
| RAP74 1–517 | $(2 \pm 0.5) \times 10^4$ | $(3.3 \pm 0.1) \times 10^{-3}$ | $(1.7 \pm 0.4) \times 10^{-7}$ |
| RAP74-NTD | $(4.6 \pm 1.9) \times 10^3$ | $(12 \pm 0.5) \times 10^{-4}$ | $(2.9 \pm 0.9) \times 10^{-7}$ |
| RAP74-CTD | $(6.8 \pm 0.8) \times 10^4$ | $(42 \pm 1.9) \times 10^{-3}$ | $(6.3 \pm 0.8) \times 10^{-7}$ |
| SRC-1 peptide | $(2.4 \pm 0.5) \times 10^2$ | $(3.3 \pm 0.1) \times 10^{-3}$ | $(1.4 \pm 0.3) \times 10^{-5}$ |

off rate and a relatively low binding affinity, with a $K_d$ of 14 $\mu$M (Figure 2D and Table 1).

*Characterization of the AR-AF1−RAP74-CTD Interaction.* The CTD of RAP74 is thought to be involved in multiple protein–protein interactions, in addition to the AR-AF1 transactivation domain (Figure 1B). The binding sites for general transcription factor TFIIB (*29*), the RNA polymerase II enzyme (*25*), and the phosphatase, FCP1 (*30, 31*), have all been mapped to the 155 C-terminal amino acids. The structure of this region has also recently been determined in both the absence (*21*) and presence of an FCP1 peptide (*22, 23*). The last 68 amino acids have been found to form a winged-helix folded domain that has been described for several DNA-binding proteins (Figure 3A). A costructure with the peptide from the FCP1 phosphatase highlights the importance of residues in helix 3 and the overall globular structure important for this binding (Figure 3A and refs *22* and *23*). To fine-map the binding of AR-AF1, the helical regions within the RAP74-CTD polypeptide were targeted for mutagenesis, with key conserved hydrophobic residues mutated to prolines to disrupt helical structure (Figure 3B). Prediction of the $\alpha$-helical structure of the RAP74-CTD polypeptide, using the primary amino acid sequence, is in good agreement with the known helical conformation of this domain (compare panels B and C of Figure 3). Therefore, using the predictions, it was possible to design mutations that would disrupt the individual $\alpha$-helices (Figure 3C). The mutations were introduced into full-length RAP74 and the RAP74-CTD polypeptide and the mutant polypeptides puri-fied by Ni-affinity chromatography (Figure 3D and data not shown). To demonstrate disruption of secondary structure elements, the wild-type and mutant RAP74 polypeptides were challenged with different proteases. Panels A and B of Figure 4 show partial protease digests for wild-type and mH1, mH2, and mH3 RAP74-CTD polypeptides with endo-Glu C protease and trypsin, respectively. It is clear that the introduction of prolines has disrupted the structure of the RAP74-CTD polypeptide with the appearance of a number of unique digestion products, or reduction in certain frag-ments, for the mutant RAP74 polypeptides (Figure 4, filled and empty arrowheads). A similar pattern of fragments for each mutant was seen with endo-Glu C digestion (Figure 4A), but with trypsin, differences were apparent between mH3 and mH1 and mH2 (Figure 4B). However, it is worth noting that the mutations did not disrupt other functions of RAP74. Thus, it was possible to reconstitute RAP30−RAP74 heteromers with both the wild-type and mutant RAP74 full-length polypeptides (data not shown). We next determined the effect of these mutations on the binding of AR-AF1. Radiolabeled RAP74-CTD wild-type or mutant polypeptides were incubated with immobilized AR-AF1, and after they had been extensively washed, the bound radioactivity was measured directly and the bound proteins were recovered for SDS−PAGE analysis. Panels A and B of Figure 5 show
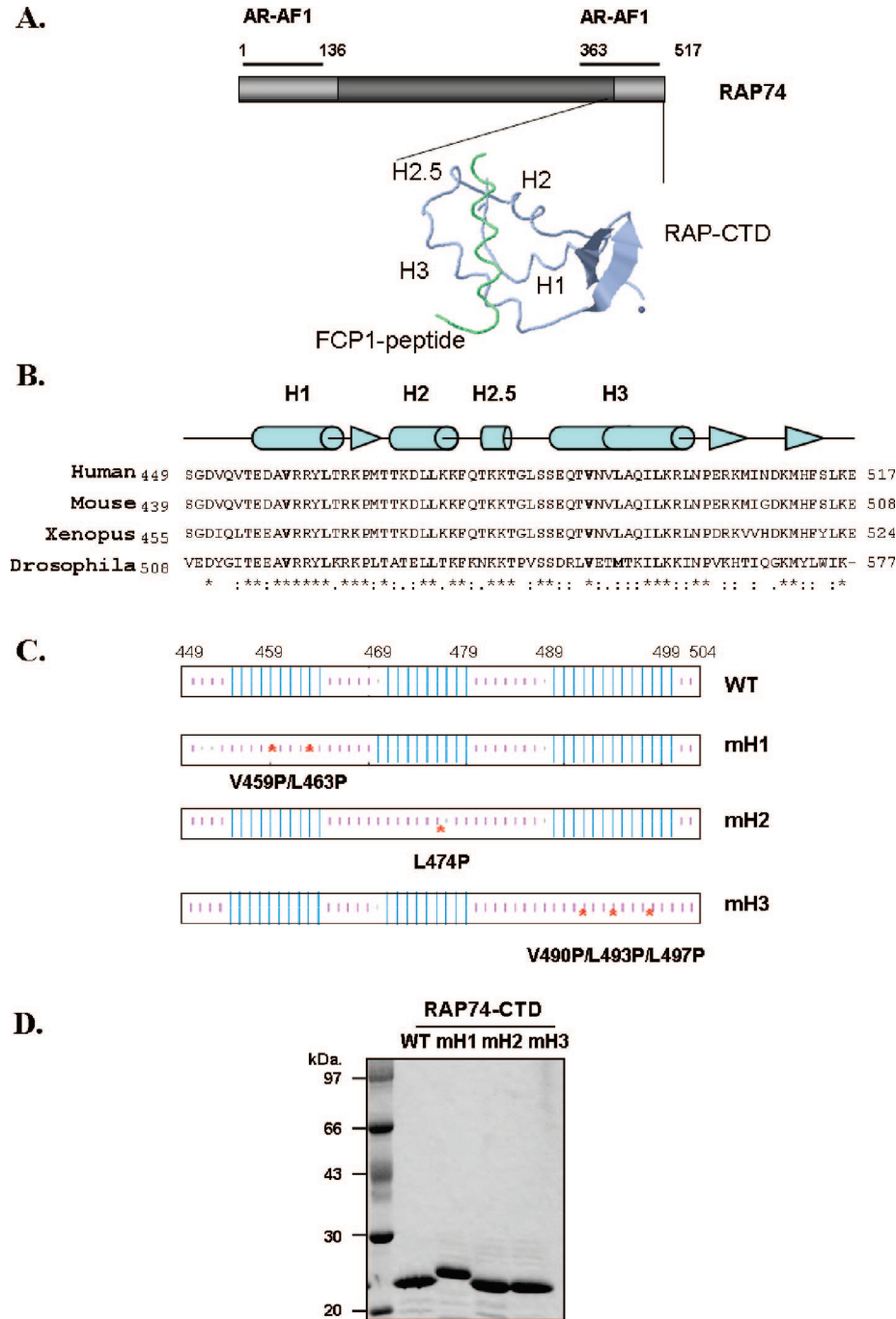
FIGURE 3: RAP74-CTD structure and mutational analysis. (A) Schematic of the large subunit of RAP74 indicating the AR-AF1 binding sites and the winged-helix structure (blue) of the 86 CTD amino acids (Protein Data Bank entry 1J2X) viewed using Cn3D. The location of the FCP1 peptide (green) is also indicated (see the text for references). (B) Species comparison of the RAP74-CTD polypeptide highlighting the conservation of hydrophobic amino acids (bold) and the location of helical segments 1, 2, and 3. GenBank accession numbers for the amino acid sequences of human, mouse, *Xenopus*, and *Drosophila* RAP74 are CAA45408, NP598562, NP001082258, and NP524246, respectively. (C) Secondary structure predictions for the wild-type and mutant polypeptides. Asterisks denote the residues mutated to proline. (D) Coomassie-stained gel showing the purification of the wild-type and mutant RAP74-CTD polypeptides. Note that mutating valine 459 and leucine 463 in helix 1 altered the mobility of the protein on SDS−PAGE (see also Figure 5C).

the binding of RAP74-CTD and full-length fragments, respectively. Disruption of each helical segment appeared to disrupt AR-AF1 binding, with the effects on the isolated CTD being the most pronounced (Figure 5A,B). Interestingly, however, when the labeled protein was recovered from AR-AF1 or the nonspecific control BSA, we observed that mutating helix 1 or 2 significantly increased the levels of nonspecific binding. In contrast, mutating helix 3 specifically reduced the level of binding to AR-AF1 without significantly altering the nonspecific binding. From these studies, we

conclude that mutating key hydrophobic residues in helix 3 in the C-terminal domain of RAP74 selectively disrupts the binding of AR-AF1.

## DISCUSSION

The ability of the AF-1 domain to participate in multiple protein–protein interactions is key to the ability of the AR to regulate gene transcription. In this study, we have characterized the binding kinetics of AR-AF1 with a component of the general
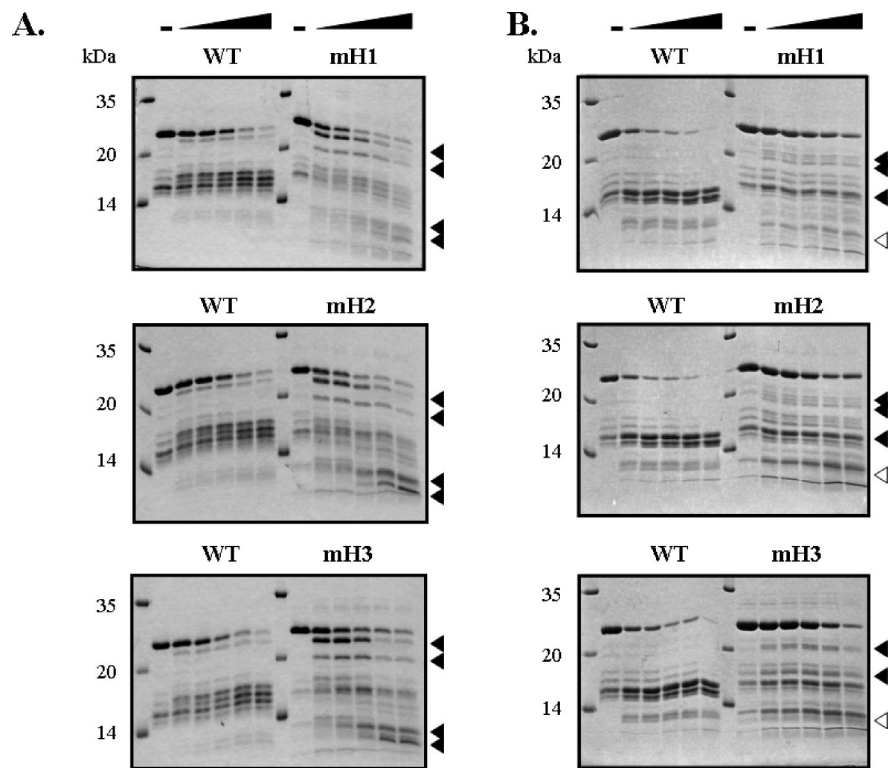
FIGURE 4: Partial proteolysis of RAP74-CTD mutant polypeptides. Wild-type or mutant polypeptides were digested with 10 ng/μL endo-Glu C protease for 2, 4, 6, 8, or 10 min (A) or 0.2 ng/μL trypsin for 1, 2, 4, 8, or 10 min (B) and the resulting fragments resolved by SDS−PAGE. The first lane for each polypeptide represents the time zero samples. Fragments selective for the different mutations relative to the wild-type polypeptide are indicated by the filled arrowheads, while digestion products reduced with the mutant polypeptides are indicated by the empty arrowheads.
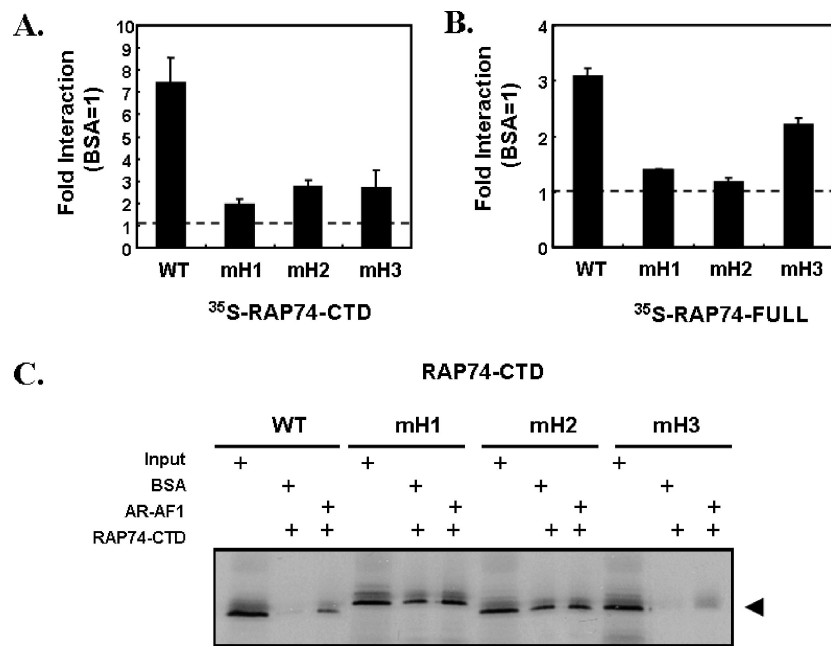


FIGURE 5: Protein–protein proximity binding assay. (A) Binding of wild-type or mutant labeled RAP74 polypeptides to AR-AF1. The level of binding is plotted relative to nonspecific interactions with BSA. The mean ± standard deviation for triplicate observations is shown. (B) As in part A, except full-length RAP74 polypeptides were analyzed. (C) SDS−PAGE of bound protein. The input (10%), nonspecific binding (BSA), and specific binding (AR-AF1) of labeled RAP74-CTD polypeptides are shown (filled arrowhead).

transcription, RAP74, and a coactivator protein SRC-1a. The structural properties of AR-AF1 that underpin its ability to participate in multiple protein–protein interactions are described in more detail elsewhere (*42*).

The binding kinetics for AR-AF1 and RAP74 polypeptides revealed $K_d$ values in the submicromolar range, while the affinity for the SRC-1 peptide was 20−80-fold lower.

Comparable affinities have been reported for the ERα-NTD (*32*) and GR-AF1 domain (*33*) binding to the general transcription factor TBP (8 and 0.19−0.25 μM, respectively) and the binding of the cochaperone protein, Bag-1L, with a subdomain of the AR-NTD (0.6 μM) (*34*). These data support a dynamic model for AR-AF1 domain folding and function involving specific protein–protein interactions and
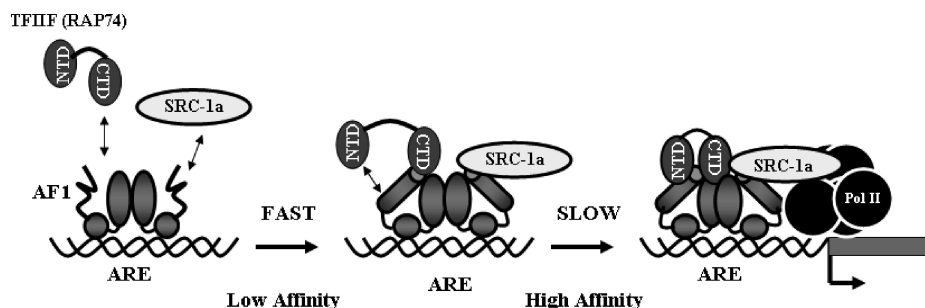
FIGURE 6: Model for AR-AF1 kinetic interactions and induced folding. TFIIF is a heterotetramer of two subunits, RAP30 and RAP74; for illustrative purposes only, the large subunit RAP74 is shown binding to one monomer of the DNA-bound AR and SRC-1 to a second. The initial interactions are proposed to be slow and of low affinity, which are followed by high-affinity binding. Interactions are associated with induced folding of the NTD; the cylinder represents an increase in α-helical structure content. Note that DNA response element binding may also result in stabilization or induced folding of the NTD (see ref *1* and references therein).

protein folding (Figure 6). In this model, initial interactions are proposed to be relatively fast but of low affinity and are followed by slower high-affinity interactions: concomitant with these interactions is the induced folding of the AF1 domain (see refs *39* and *42*). A similar model has been proposed for acidic activator−target protein interactions (*35*).

Extensive chromatin immunoprecipitation studies at the prostate-specific antigen (PSA) gene have revealed the binding of both the AR and members of the p160 coactivator family at the promoter and enhancer sequences (*36–38*). We have confirmed that the AR predominantly occupies ARE III (positions −4200 to −3872) but is also observed binding to ARE I (positions −370 to −416) and ARE II (positions −594 to −291). Significantly, we also observed binding of TFIIF at ARE III together with RNA polymerase II, although both components of the general transcription machinery were predominantly located at the ARE I and ARE II promoter region (D. N. Lavery and I. J. McEwan, unpublished observations). These results together with our previous in vitro studies (*6*) support the involvement of AR-AF1−TFIIF interactions in the assembly of the preinitiation complex (PIC) and transcription initiation.

Several high-resolution structures of RAP74 and RAP30 have been published recently. N-terminal regions of both RAP30 (amino acids 2–119) and RAP74 (amino acids 2–172) were cocrystallized at 1.7 Å resolution. These subunits dimerize via their N-terminal domains in a novel "triple-barrel" fold with pseudo-2-fold symmetry (*20*). It is apparent that the C-terminal domain (amino acids 363–517) of RAP74 forms a tight globular domain with three α-helices followed by an antiparallel β-sheet (*21*). This domain was further characterized in a complex with the Pol II CTD-associated phosphatase Fcp1 by both NMR spectroscopy and X-ray crystallography. From these studies, it appears that Fcp1 interacts with RAP74 by binding a shallow groove generated by helices 2 and 3 of the general transcription factor in a manner similar to that of the TFIIB−Fcp1 interaction (*22, 23*). The FCP1 peptide made hydrophobic interactions with residues in helix 2 and strand 2, but primarily with Val 490, Leu 493, and Leu 497 in helix 3. It is interesting, therefore, that mutation of these residues also selectively disrupted the binding of AR-AF1.

The conformation of AR-AF1 appears to be adaptive and to share properties with a "collapsed disordered conformation", which is distinct from fully unfolded or folded structures (*42*). We have previously demonstrated the presence of putative helical regions and shown the increase in

α-helix content upon binding of the TFIIF RAP74 subunit (*24, 39*). It seems reasonable to speculate that this increase in the level of helical structure results in the formation of α-helix, which would occupy the groove on the RAP74-CTD polypeptide, in a manner similar to that of FCP1 binding. This would suggest that the binding of AR-AF1 and FCP1 to TFIIF would be mutually exclusive. However, Jänne and co-workers recently identified an FCP1 family member, small carboxyl-terminal domain phosphatase 2 (SCP2), as an interacting partner for the AR-NTD (*40*). SCP2 was recruited to the PSA gene and attenuated androgen-dependent gene transcription. It therefore remains formally possible that AR–TFIIF–FCP1 forms a multisubunit complex.

In addition to protein–protein interactions, the RAP74-CTD polypeptide has been proposed to interact with DNA. Interestingly, in a series of cross-linking experiments, TFIIF was shown to alter the architecture of the DNA-PIC and so facilitate open complex formation and initiation of RNA synthesis (*41*). Thus, interactions of AR-AF1 with TFIIF (RAP74) may compete for binding of FCP1 to TFIIF and/or the interactions of the RAP74-CTD polypeptide with DNA, to ensure phosphorylation of the CTD of RNA polymerase II large subunit and subsequent release of the polymerase from the preinitiation complex and conversion to the elongation form. Further experiments will be required to test this hypothesis directly.

## REFERENCES

1. Lavery, D. N., and McEwan, I. J. (2005) Structure and Function of Steroid Receptor AF1 Transactivation Domains: Induction of Active Conformations. *Biochem. J. 391*, 449–464.
2. Simental, J. A., Sar, M., Lane, M. V., French, F. S., and Wilson, E. M. (1991) Transcriptional Activation and Nuclear Targeting Signals of the Human Androgen Receptor. *J. Biol. Chem. 266*, 510–518.
3. Jenster, G., van der Korput, H. A., Trapman, J., and Brinkmann, A. O. (1995) Identification of Two Transcription Activation Units in the N-Terminal Domain of the Human Androgen Receptor. *J. Biol. Chem. 270*, 7341–7346.
4. Chamberlain, N. L., Whitacre, D. C., and Miesfeld, R. L. (1996) Delineation of Two Distinct Type 1 Activation Functions in the Androgen Receptor Amino-Terminal Domain. *J. Biol. Chem. 271*, 26772–26778.
5. McEwan, I. J., and Gustafsson, J. (1997) Interaction of the Human Androgen Receptor Transactivation Function with the General Transcription Factor TFIIF. *Proc. Natl. Acad. Sci. U.S.A. 94*, 8485–8490.
6. Choudhry, M. A., Ball, A., and McEwan, I. J. (2006) The Role of the General Transcription Factor IIF in Androgen Receptor-Dependent Transcription. *Mol. Endocrinol. 20*, 2052–2061.

7. Ikonen, T., Palvimo, J. J., and Janne, O. A. (1997) Interaction between the Amino- and Carboxyl-Terminal Regions of the Rat Androgen Receptor Modulates Transcriptional Activity and is Influenced by Nuclear Receptor Coactivators. *J. Biol. Chem. 272*, 29821–29828.

8. Aarnisalo, P., Palvimo, J. J., and Janne, O. A. (1998) CREB-Binding Protein in Androgen Receptor-Mediated Signaling. *Proc. Natl. Acad. Sci. U.S.A. 95*, 2122–2127.

9. Fronsdal, K., Engedal, N., Slagsvold, T., and Saatcioglu, F. (1998) CREB Binding Protein is a Coactivator for the Androgen Receptor and Mediates Cross-Talk with AP-1. *J. Biol. Chem. 273*, 31853–31859.

10. Alen, P., Claessens, F., Verhoeven, G., Rombauts, W., and Peeters, B. (1999) The Androgen Receptor Amino-Terminal Domain Plays a Key Role in p160 Coactivator-Stimulated Gene Transcription. *Mol. Cell. Biol. 19*, 6085–6097.

11. Bevan, C. L., Hoare, S., Claessens, F., Heery, D. M., and Parker, M. G. (1999) The AF1 and AF2 Domains of the Androgen Receptor Interact with Distinct Regions of SRC1. *Mol. Cell. Biol. 19*, 8383–8392.

12. Ma, H., Hong, H., Huang, S. M., Irvine, R. A., Webb, P., Kushner, P. J., Coetzee, G. A., and Stallcup, M. R. (1999) Multiple Signal Input and Output Domains of the 160-Kilodalton Nuclear Receptor Coactivator Proteins. *Mol. Cell. Biol. 19*, 6164–6173.

13. Reid, J., Murray, I., Watt, K., Betney, R., and McEwan, I. J. (2002) The Androgen Receptor Interacts with Multiple Regions of the Large Subunit of General Transcription Factor TFIIF. *J. Biol. Chem. 277*, 41247–41253.

14. Lee, D. K., Duan, H. O., and Chang, C. (2000) From Androgen Receptor to the General Transcription Factor TFIIH. Identification of Cdk Activating Kinase (CAK) as an Androgen Receptor NH2-Terminal Associated Coactivator. *J. Biol. Chem. 275*, 9308–9313.

15. Dotzlaw, H., Moehren, U., Mink, S., Cato, A. C., Iniguez Lluhi, J. A., and Baniahmad, A. (2002) The Amino Terminus of the Human AR is Target for Corepressor Action and Antihormone Agonism. *Mol. Endocrinol. 16*, 661–673.

16. Belandia, B., Powell, S. M., Garcia-Pedrero, J. M., Walker, M. M., Bevan, C. L., and Parker, M. G. (2005) Hey1, a Mediator of Notch Signaling, is an Androgen Receptor Corepressor. *Mol. Cell. Biol. 25*, 1425–1436.

17. Lei, L., Ren, D., Finkelstein, A., and Burton, Z. F. (1998) Functions of the N- and C-Terminal Domains of Human RAP74 in Transcriptional Initiation, Elongation, and Recycling of RNA Polymerase II. *Mol. Cell. Biol. 18*, 2130–2142.

18. Lei, L., Ren, D., and Burton, Z. F. (1999) The RAP74 Subunit of Human Transcription Factor IIF has Similar Roles in Initiation and Elongation. *Mol. Cell. Biol. 19*, 8372–8382.

19. Yan, Q., Moreland, R. J., Conaway, J. W., and Conaway, R. C. (1999) Dual Roles for Transcription Factor IIF in Promoter Escape by RNA Polymerase II. *J. Biol. Chem. 274*, 35668–35675.

20. Gaiser, F., Tan, S., and Richmond, T. J. (2000) Novel Dimerization Fold of RAP30/RAP74 in Human TFIIF at 1.7 Å Resolution. *J. Mol. Biol. 302*, 1119–1127.

21. Kamada, K., De Angelis, J., Roeder, R. G., and Burley, S. K. (2001) Crystal Structure of the C-Terminal Domain of the RAP74 Subunit of Human Transcription Factor IIF. *Proc. Natl. Acad. Sci. U.S.A. 98*, 3115–3120.

22. Kamada, K., Roeder, R. G., and Burley, S. K. (2003) Molecular Mechanism of Recruitment of TFIIF: Associating RNA Polymerase C-Terminal Domain Phosphatase (FCP1) by Transcription Factor IIF. *Proc. Natl. Acad. Sci. U.S.A. 100*, 2296–2299.

23. Nguyen, B. D., Abbott, K. L., Potempa, K., Kobor, M. S., Archambault, J., Greenblatt, J., Legault, P., and Omichinski, J. G. (2003) NMR Structure of a Complex Containing the TFIIF Subunit RAP74 and the RNA Polymerase II Carboxyl-Terminal Domain Phosphatase FCP1. *Proc. Natl. Acad. Sci. U.S.A. 100*, 5688–5693.

24. Reid, J., Kelly, S. M., Watt, K., Price, N. C., and McEwan, I. J. (2002) Conformational Analysis of the Androgen Receptor Amino-Terminal Domain Involved in Transactivation. Influence of Structure-Stabilizing Solutes and Protein-Protein Interactions. *J. Biol. Chem. 277*, 20079–20086.

25. Wang, B. Q., and Burton, Z. F. (1995) Functional Domains of Human RAP74 Including a Masked Polymerase Binding Domain. *J. Biol. Chem. 270*, 27035–27044.

26. Combet, C., Blanchet, C., Geourjon, C., and Deleage, G. (2000) NPS@: Network Protein Sequence Analysis. *Trends Biochem. Sci. 25*, 147–150.

27. Christiaens, V., Bevan, C. L., Callewaert, L., Haelens, A., Verrijdt, G., Rombauts, W., and Claessens, F. (2002) Characterization of the Two Coactivator-Interacting Surfaces of the Androgen Receptor and their Relative Role in Transcriptional Control. *J. Biol. Chem. 277*, 49230–49237.

28. Callewaert, L., Verrijdt, G., Christiaens, V., Haelens, A., and Claessens, F. (2003) Dual Function of an Amino-Terminal Amphipatic Helix in Androgen Receptor-Mediated Transactivation through Specific and Nonspecific Response Elements. *J. Biol. Chem. 278*, 8212–8218.

29. Fang, S. M., and Burton, Z. F. (1996) RNA Polymerase II-Associated Protein (RAP) 74 Binds Transcription Factor (TF) IIB and Blocks TFIIB-RAP30 Binding. *J. Biol. Chem. 271*, 11703–11709.

30. Archambault, J., Pan, G., Dahmus, G. K., Cartier, M., Marshall, N., Zhang, S., Dahmus, M. E., and Greenblatt, J. (1998) FCP1, the RAP74-Interacting Subunit of a Human Protein Phosphatase that Dephosphorylates the Carboxyl-Terminal Domain of RNA Polymerase IIO. *J. Biol. Chem. 273*, 27593–27601.

31. Kobor, M. S., Simon, L. D., Omichinski, J., Zhong, G., Archambault, J., and Greenblatt, J. (2000) A Motif Shared by TFIIF and TFIIB Mediates their Interaction with the RNA Polymerase II Carboxy-Terminal Domain Phosphatase Fcp1p in *Saccharomyces cerevisiae*. *Mol. Cell. Biol. 20*, 7438–7449.

32. Warnmark, A., Wikstrom, A., Wright, A. P., Gustafsson, J. A., and Hard, T. (2001) The N-Terminal Regions of Estrogen Receptor α and β are Unstructured in Vitro and show Different TBP Binding Properties. *J. Biol. Chem. 276*, 45939–45944.

33. Copik, A. J., Webb, M. S., Miller, A. L., Wang, Y., Kumar, R., and Thompson, E. B. (2006) Activation Function 1 of Glucocorticoid Receptor Binds TATA-Binding Protein in Vitro and in Vivo. *Mol. Endocrinol. 20*, 1218–1230.

34. Shatkina, L., Mink, S., Rogatsch, H., Klocker, H., Langer, G., Nestl, A., and Cato, A. C. (2003) The Cochaperone Bag-1L Enhances Androgen Receptor Action Via Interaction with the NH2-Terminal Region of the Receptor. *Mol. Cell. Biol. 23*, 7189–7197.

35. Hermann, S., Berndt, K. D., and Wright, A. P. (2001) How Transcriptional Activators Bind Target Proteins. *J. Biol. Chem. 276*, 40127–40132.

36. Shang, Y., Myers, M., and Brown, M. (2002) Formation of the Androgen Receptor Transcription Complex. *Mol. Cell 9*, 601–610.

37. Louie, M. C., Yang, H. Q., Ma, A. H., Xu, W., Zou, J. X., Kung, H. J., and Chen, H. W. (2003) Androgen-Induced Recruitment of RNA Polymerase II to a Nuclear Receptor-p160 Coactivator Complex. *Proc. Natl. Acad. Sci. U.S.A. 100*, 2226–2230.

38. Kang, Z., Janne, O. A., and Palvimo, J. J. (2004) Coregulator Recruitment and Histone Modifications in Transcriptional Regulation by the Androgen Receptor. *Mol. Endocrinol. 18*, 2633–2648.

39. Kumar, R., Betney, R., Li, J., Thompson, E. B., and McEwan, I. J. (2004) Induced α-Helix Structure in AF1 of the Androgen Receptor upon Binding Transcription Factor TFIIF. *Biochemistry 43*, 3008–3013.

40. Thompson, J., Lepikhova, T., Teixido-Travesa, N., Whitehead, M. A., Palvimo, J. J., and Jänne, O. A. (2006) Small carboxyl-terminal phosphatase 2 attenuates androgen-dependent transcription. *EMBO J. 25*, 2757–2767.

41. Robert, F., Douziech, M., Forget, D., Egly, J. M., Greenblatt, J., Burton, Z. F., and Coulombe, B. (1998) Wrapping of Promoter DNA Around the RNA Polymerase II Initiation Complex Induced by TFIIF. *Mol. Cell 2*, 341–351.

42. Lavery, D. N., and McEwan, I. J. (2008) Structural characterization of the native NH2-terminal transactivation domain of the human androgen receptor: A collapsed disordered conformation underlies structural plasticity and protein-induced folding. *Biochemistry 47*, 3360–3369.